LBL-28025
Preprint

Lawrence Berkeley Laboratory
UNIVERSITY OF CALIFORNIA

Physics Division

Submitted to Astrophysical Journal

The Temperature of the Cosmic Background Radiation: Results from the 1987 and 1988 Measurements at 3.8 GHz

G. De Amici, M. Bensadoun, M. Bersanelli, A. Kogut,
S. Levin, G.F. Smoot, and C. Witebsky

November 1989

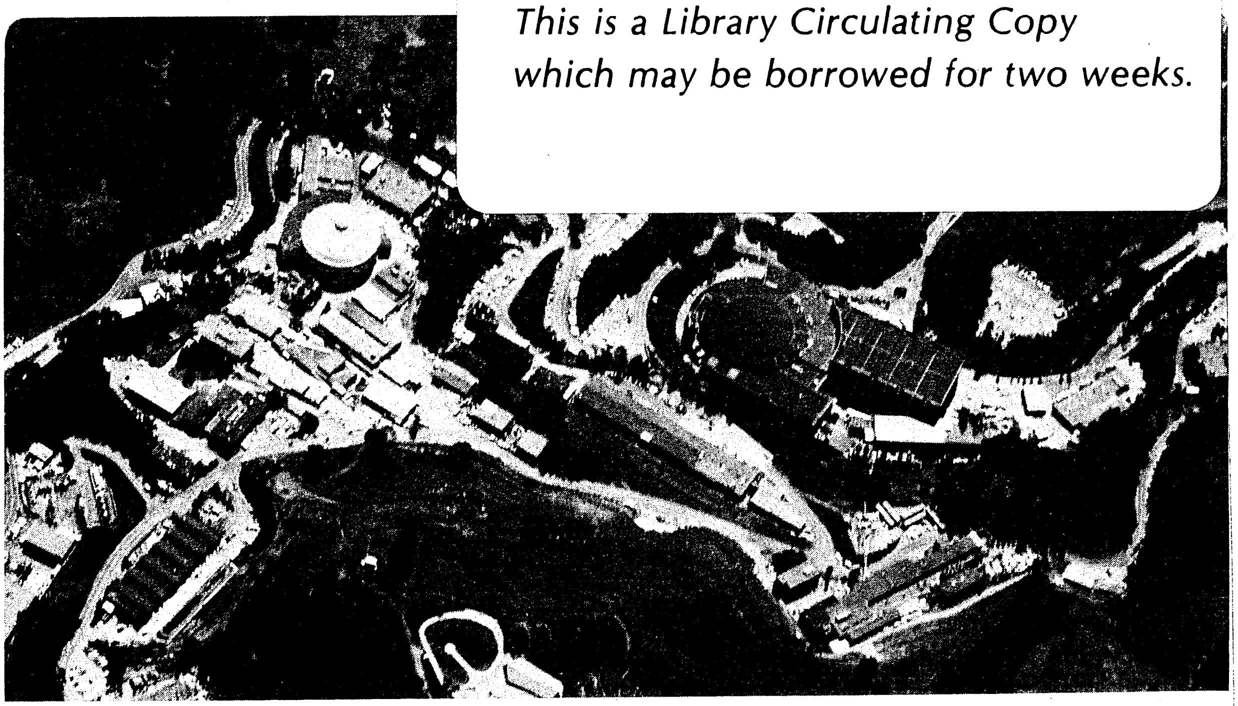

Prepared for the U.S. Department of Energy under Contract Number DE-AC03-76SF00098.

LBL-28025

The Temperature of the Cosmic Background Radiation: Results from the 1987 and 1988 Measurements at 3.8 GHz

G. De Amici, M. Bensadoun, M. Bersanelli, A. Kogut, S. Levin, G.F. Smoot, and C. Witebsky

Lawrence Berkeley Laboratory
and Space Sciences Laboratory
University of California
Berkeley, CA 94720

November 1989

This work was supported by the Director, Office of Energy Research, Office of High Energy and Nuclear Physics, Division of High Energy Physics of the U. S. Department of Energy under Contract No. DE-AC03-76SF00098, and by the National Science Foundation Grant No. AST 8406187.

The Temperature of the Cosmic Background Radiation: Results from the 1987 and 1988 Measurements at 3.8 GHz

Giovanni De Amici, Marc Bensadoun, Marco Bersanelli,
Al Kogut, Steve Levin, George F. Smoot, Chris Witebsky

Space Sciences Laboratory and Lawrence Berkeley Laboratory,
University of California, Berkeley, USA

ABSTRACT

We have measured the temperature of the cosmic background radiation (CBR) at a frequency of 3.8 GHz (7.9 cm wavelength), during two consecutive summers, obtaining a brightness temperature, T_{CBR}, of 2.56±0.08 K in 1987 and 2.71±0.07 K in 1988 (68% confidence level). The new results are in agreement with our previous measurement at 3.7 GHz obtained in 1986, and have smaller error bars. Combining measurements from all three years we obtain T_{CBR} = 2.64±0.07 K.

subject headings: cosmic background radiation

I. INTRODUCTION

The low-frequency (Rayleigh-Jeans) spectrum of the cosmic background radiation (CBR) is expected to contain information relevant to the physical processes that occurred in the early universe (Danese and De Zotti 1982, and references therein). The recent detection of a radiation excess in the Wien region (Matsumoto *et al.* 1988) can be explained either with a Compton distortion of the spectrum at the high frequencies, which would entail a distortion also at low frequencies, or with a previously undetected component of the radiation background (Hayakawa *et al. 1987*, Smoot *et al* 1988). A precise measurement of the shape of the spectrum at the low frequencies would help to discriminate between the two possibilities. We choose to observe at 3.8 GHz because at frequencies above 2 GHz the galactic background emission is smaller than the CBR signal, making the measurement easier to perform, while the atmospheric signal is predicted to be stable and small (about 1 K) below 20 GHz. These two facts define the 2-18 GHz range as the best frequency window for ground based receivers. The commercial use of the 3.7-4.2 GHz bandwidth for popular direct-broadcast television has made high-performance receivers in this frequency band easily and cheaply available.

Our group in Berkeley has been involved in designing and performing high-precision, ground based measurements of the low-frequency spectrum of the CBR since 1980; previous results from measurements by us and our collaborators at 2.5, 4.75, 10, 33 and 90 GHz have greatly improved the accuracy of the spectral data in the Rayleigh-Jeans region (e.g. Smoot *et al.*1985, 1987, De Zotti 1986). The measurements reported here constitute the second and third year effort with a receiver working in the 3.5-4 GHz frequency band.

A previous paper (De Amici *et al.* 1988) reported on the results of our first year observations at 3.7 GHz.

Footnote:

Unless otherwise specified, all error bars given in this paper are 68% confidence level limits (1-σ level).

II. MEASUREMENT CONCEPT

Our radiometer is a microwave receiver whose output signal, S, is proportional to the input power, P, per unit bandwidth, B, and is measured in units of antenna temperature, T_A. For a blackbody at a thermodynamic temperature T covering the aperture of the antenna:

$$T_A = \frac{P}{kB} = \frac{T_\nu}{e^{T_\nu/T} - 1} \tag{1}$$

where $T_\nu = h\nu/k$ ($\approx$ 0.183 K at 3.8 GHz), h is Planck's constant, ν is frequency, and k is Boltzmann's constant.

When the receiver is pointed at the zenith, the antenna temperature, $T_{A,zenith}$, is the sum of many contributions:

$$T_{A,zenith} = T_{A,CBR} + T_{A,galaxy} + T_{A,ground} + T_{A,atm} \tag{2}$$

where the attenuation due to the atmosphere ($\approx$ 0.3%) has been neglected in this discussion, but not in the analysis, and $T_{A,CBR}$, $T_{A,galaxy}$, $T_{A,ground}$, and $T_{A,atm}$ are respectively the antenna temperatures of the CBR, the galaxy, the ground seen through the antenna sidelobes, and the atmosphere. Each measurement compares the antenna temperature of the zenith sky with that of a reference cold load. The difference in radiometer output when comparing the sky and the cold load is:

$$G\,(S_{zenith} - S_{load}) = T_{A,zenith} - T_{A,load} + \Delta T_{sys} + \frac{\Delta G}{G}(T_{A,load} + T_{sys}) + \frac{\Delta R}{R}(T_{sys} - T_{A,load}) + \frac{\Delta L}{L}(T_{sys} - T_{A,load}) \tag{3}$$

where G is the calibration coefficient of the receiver, S is the output signal when viewing the zenith or the cold load, $\Delta G/G$ represents the fractional change in calibration coefficient, $\Delta R/R$ is the fractional change in reflection coefficient of the horn and amplifier, $\Delta L/L$ is the fractional change in insertion loss of the antenna, T_{sys} is the system temperature of the receiver, and ΔT_{sys} is the position-dependent change in receiver system temperature. Changes in insertion loss and reflection coefficient in the antenna affect the net power going through it (i.e. the difference between the input load temperature and the broadcast system temperature). The last five terms in eq. (3) can be evaluated by rotating the radiometer, and looking at its output with warm and cold loads.

However, we were unable to make a stable cold load that can be rotated with the radiometer. A warm load alone does not allow us to differentiate between changes in system temperature and calibration constant. In any case when an ambiguity was possible, we assumed a worst case scenario. As will be shown later, the last terms in eq. (3) are almost negligible for this radiometer.

III. INSTRUMENT DESCRIPTION

The instrument used for this experiment is a total power, direct RF-gain radiometer. The relevant parameters are given in Table 1. The instrument used in 1987 and 1988 was similar to the radiometer used in 1986, (De Amici *et al.* 1988). In 1987 the highpass filter was replaced by a bandpass filter, which better defines the radiometer's frequency range, and rejects almost all of the radio-frequency interference (RFI) that affected the experiment in 1986. A new second amplifier, of higher gain and better thermal and mechanical stability was used. The increased gain allowed us to put attenuation between the active components of the RF circuit, to improve the impedance match. A new detector diode shows less saturation at the operating signal levels. The DC amplifier was modified, so that its gain can be controlled via an external switch; this allowed us to minimize the effects of digitization noise in the analog/digital converter.

In order to reduce the effect of possible localized non-linearities in the ADC, we tried to take full advantage of the dynamic range available by switching the gain of the DC amplifier between two different settings; a "low" gain setting whose full-scale limit accomodates the signal from an ambient temperature load, and a "high" gain one that can only accommodate a load at or below liquid nitrogen (LN_2) temperature (77K). Measurements of the calibration coefficient of the radiometer were made in the "low" settings, while measurements of the atmospheric and zenith sky signals were done in the "high" setting. The ratio between "high" and "low" was measured many times during the data taking nights; it was 3.750±0.028 in 1987. In 1988, with modifications to the DC amplifier, it became 2.197±0.011.

The center frequency and equivalent bandwidth of the radiometer are defined by the band-pass filter, which has a center frequency of 3.8 GHz and a 3 dB passband of ±100 MHz, and by the frequency-dependent gain of the amplifiers.

The DC amplifier was tuned to show a null offset for a terminated input.

In 1988 we inserted an attenuator before the detector diode and proportionally increased the gain of the DC amplifier. This change substantially improved the radiometer linearity: tests with different temperature loads showed a -1.8±0.1% change in the radiometer output for a ≈ 300K load, and a -0.14±0.01% change for a 4K load.

IV. MEASURING SITE

The experiment was carried out from the Nello Pace Laboratory of the University of California's White Mountain Research Station. The Laboratory lies on a mountain plateau, 3800 meters above sea level, at a latitude of 37.6° N. The area is in the rain shadow of the Sierra Nevada mountain range in eastern California. Typical atmospheric precipitable water content (the dominant source of variability in atmospheric antenna temperature) at the site is less than 5 mm during clear summer nights. Data with the cold load at liquid helium (LHe) temperature were taken during the nights of 14 and 15 Sept 1987 (UT), and of 16, 17, and 19 September 1988 (UT). In the same period, our group operated radiometers at 90, 10.0 (in 1987 only), 7.5 (in 1988 only), and 1.5 GHz; results from those experiments have been reported by Levin *et al* (1989) and by Kogut *et al* (1989, Ap.J.).

V. GALACTIC MEASUREMENTS

The galactic signal at 3.8 GHz contributes between 40 mK and 300 mK to the total sky brightness. Because of the galactic emission profile, it is desirable to conduct our measurements of the CBR at R.A. between 120° and 230°, when the galactic emission is both low (about 40 mK) and constant with time (changing by less than 10 mK over a 7 hour period); this can be accomplished only by making our measurements either during the day in the summer or during the night in the winter, when the Research Station is inaccessible to heavy equipment. We compromised by taking our data at times when the galactic disk is at least 20° away from the zenith, and by directly measuring the galactic emission profile.

Galactic measurements compared the signal from the sky at 15° from zenith toward the East and West directions (the pointing angles were 15°10' E and 14°44' W respectively and repeatable to 5' throughout the night). The radiometer was moved every 32 seconds, so that a complete observation took 64 sec. Approximately every hour, the measurement sequence was interrupted and the radiometer was calibrated with a warm target. A measurement typically lasted 4-6 hours.

The differential measurement technique simplifies data analysis in several ways. Since the zenith angles are equal, any zeroth-order uncertainty due to atmospheric signal is removed. Because of the small zenith angle, the ground contribution is small (0.002±0.005 K toward East, and 0.008±0.005 K toward West), and the differential character of the measurement makes gain variation comparatively unimportant.

This technique only measures the difference in the galactic signal, and therefore does not provide direct information on the absolute level of galactic emission. It is still useful, however, since the results can be compared to the galactic profile estimated from the model, and used to verify its accuracy.

We made a two-component model of the galactic emission, using the low-frequency maps by Haslam *et al.* (1982), and adding a compilation of known HII regions. The map was convolved to our antenna beam pattern and scaled in frequency with spectral index of 2.75 for the synchrotron radiation and 2.1 for the thermal emission. Figure 1 shows the results of our scans from 1987, superimposed on the prediction of the model. Each experimental point is the combination of the data from different nights, averaged in 5-minute wide bins.

The agreement between the model and the data is quite good; the average difference is 0.002 (±0.007) K, with a peak-to-peak spread of about 0.05 K. Most of the discrepancy comes from measurements made in the early morning (11-15 h UT), when the data were contaminated by the presence of the almost full Moon in or close to the beam. The difference between measured and predicted galactic signal could be due to a residual error after subtraction of the selenic emission, or to an inadequacy of the model in representing the emission from regions close to the plane of the galaxy. Residual r.m.s. scatter, uncertainties in the measured antenna beam pattern and uncertainties in the original data used for the model suggest that the galactic correction during CBR measurements is not known to better than 0.01 K, with 75% of this uncertainty being related to uncertainties in the zero level of the data we used in our model, and the remainder to discrepancies between the data and the model. We use 0.010 K for the galaxy-induced uncertainty on absolute (CBR) measurements, and 0.005-0.008 K for differential (atmospheric emission) measurements with beam spacings of 30° and 40°.

VI. ATMOSPHERIC MEASUREMENTS

The atmospheric signal was measured by tipping the radiometer to different directions and comparing the signal received when pointing to a given zenith angle to the signal received when pointing to the zenith.

Atmospheric measurements were made as close in time as possible to measurements of the zenith sky temperature; whenever possible, we coordinated with the other radiometers, so as to have simultaneous measurements at all frequencies.

a) Experimental technique

Each measurement consisted of a few (usually 8) scans; one scan involves pointing the receiver, in order, toward the 40W, 30W, zenith, 30E, and 40E positions. Between each pair of scans, and both at the beginning and at the end of each measurement, the radiometer was calibrated by comparing the signal from the sky with the signal from an ambient temperature load. Table 2 shows the succession of positions and targets during a scan.

Occasionally, warm eccosorb was used also at the 30° and 40° positions (both in the East and West directions), to check that the radiometer gain stayed constant throughout the different positions. The precision and repeatability of the pointing angles were controlled by measuring them with a bubble clinometer many times throughout the experiment; the values for the angles are given in table 3, and were repeatable within 7'. Each scan yielded an atmospheric temperature for each of the four angles away from the zenith. Statistical uncertainty in the measured atmospheric signal is twice as large for the 30° values as for the 40° ones; total uncertainty (which is dominated by systematics) scales in a similar way. The higher western horizon induces a large sidelobe correction in the 40W data. The four values from each scan were averaged together with weight inversely proportional to the statistical uncertainty; the average constitutes the result of a scan. The scans were then averaged together to give a value for a measurement.

The results of all atmospheric measurements are reported in Table 4. The average (with statistical error only) is 0.898±0.012 K in 1987, and 0.959±0.008 K in 1988.

b) *Statistical errors*

The errors listed in Table 4 are the statistical error of the individual measurements, caused by random spread of the results of the scans. Digitization problems in the ADC could boost or reduce this spread in an uncontrolled way; to avoid this, we increased the gain of the DC amplifier, so that the spread left in the data is dominated by noise in the RF section of the radiometer, by short term variations in the atmospheric emission, or by changes in the gain of the receiver. During a measurement, the data are quite consistent with each other, and the statistical error is small; however, when different measurements are compared, the difference is twice as large as the r.m.s. error of a single measurement.

- 1987 data -

The average of all measurements (as reported in Table 4a) gives $T_{A,atm}$ = 0.898 K with an r.m.s. of 0.037 K. This is slightly larger than the spread in the data expected from computations based on atmospheric models; under fair weather conditions the atmospheric emission is generally expected to be stable with time at 3.8 GHz. However, the weather conditions during our data-taking nights, and especially during the night of 14 September, when the first two LHe runs were done, were extremely poor and variable.

For the analysis of the second and third LHe run, we will use the value of atmospheric emission that had been directly measured immediately before or after the run (see table 4a); for the first LHe run, we used the 10 GHz data to evaluate the water vapour content of the atmosphere at different times. Then we computed the atmospheric temperature at 3.8 GHz during one of our measurement, and obtained a ratio (model to data) of 0.92. We used this value to correct the atmospheric temperature predicted by the model during the first LHe run.

The extrapolation yields $T_{A,atm} = 0.97 \pm 0.07$ K.

- 1988 data -

In 1988 the weather pattern was more favorable; the average of all measurements is 0.959 K, with a 0.007 K statistical error.

c) *Systematic errors*

Other possible errors in our measurements are caused by the atmospheric and galactic models we use, by an incorrect subtraction of the sidelobe contribution, by the size of the antenna beam, by the pointing of the antenna, by the correction to the data as induced by saturation in the receiver, by position-dependent changes in the gain or the offset, and by uncertainties in the value of the receiver's calibration constant. These uncertainties cannot be reduced simply by taking more data. Table 5 summarizes the contribution of each element. Systematic errors that were not significantly modified with respect to the 1986 experiment are only briefly discussed here.

The problem of radio frequency interference (RFI) is intrinsic to the design of this receiver. Geosynchronous satellite transmitters are localized around the celestial equator. Ground based and airborne radars, which caused problems in 1986, operate above 4.2 GHz, and have been eliminated by narrowing the acceptance band of the radiometer. Airplanes flew over our site in 1987 and 1988, but data taken at those times show no difference (within the uncertainty caused by system noise, ±0.003 K for an overflight lasting about 30 seconds) from nearby data. The effect of ground-based microwave links is unknown. We observed the frequency spectrum of the received signal a few days before and after the data-taking nights; no RFI signal was detected at the 0.002 K level. Although this test does not detect RFI that is present as many low-level signals, or transmitters that are active only occasionally, it is a strong indication that RFI was not present.

Ground-emitted and stray radiation pickup through the sidelobes of the antenna were reduced by the use of an antenna of high directivity. To that we added ground screens; large wooden frames covered with fine aluminum net were erected around the radiometer. The screens redirected to the sky the parts of the antenna beam which would otherwise have seen the ground. We checked their effectiveness by temporarily extending them, adding layers of ground screens which would be impractical to use during the entire experiment. The extra screens were then taken down, and the signal difference is a measure of the remaining ground contribution. We repeated the procedure until the last extension did not produce any measurable change in signal. We measured a sidelobe contribution of 0.007±0.004 K when looking to the zenith; looking to the East we got 0.010±0.006 at 30°, and 0.020±0.008 at 40°, while to the West, where the local horizon is quite higher, we got 0.015±0.007 at 30°, and 0.035±0.010 at 40°, with negligible (less than 0.005 K) changes from 1987 to 1988. These measurements are within uncertainty from the results of modelling the ground as seen by diffraction over the shields. The data have been corrected for this effect, and the uncertainties (added in quadrature) taken as the uncertainty of the correction.

The calibration coefficient G is measured from the difference in signal between two loads at widely different and well known temperatures (usually an ambient and a cold target), after allowing for saturation effects in the amplification and detection chain. The timescale of the measurements is such that drifts in gain, measured to be less than 0.1% over a 17-minute time period when the radiometer was looking at a thermally-isolated ambient temperature piece of eccosorb, could become a problem. Measurements of the gain were done before each scan; the measured values show a linear dependence with time; after allowing for this dependence, the residual variation in the gain is less than 10^{-5} over the duration of a scan. Errors in measurement of the calibration coefficient, which amount to 0.8% in 1987 and 0.6% in 1988, are dominated by the uncertainty in the ratio between "high" and "low" gain. The gain ratio was measured by looking at two loads (zenith sky and a piece of cardboard) with the radiometer in each gain level. The measurement was repeated at least twice a night, giving a ratio of 3.750 ± 0.028; for a fractional error of 0.75%. There is no indication of systematic differences from night to night. Combining the errors in quadrature gives a 0.78% uncertainty, which, for $T_{A,atm} \approx 0.9$ K, results in an error of less than 0.007 K.

The uncertainty introduced by saturation effects in the detector diode in 1987 was reduced by the use of a different detector in 1988. The correction due to saturation for the ambient temperature (280 K) load that we use as warm calibrator, is 1.8±0.1%. The uncertainty resulting in $T_{A,atm}$ from this correction is ±0.010 K.

Errors in the value of the calibration coefficient affect the atmospheric antenna temperature by less than 0.003 K. If instead the calibration coefficient were to change its value during a measurement, then an uncertainty as small as 0.1% would become a ±0.085 K uncertainty in the measured quantity. We measured the calibration coefficient before and after each scan, and extrapolated linearly between scans. We took as error on the calibration coefficient the difference between a best fit interpolation through all the values obtained during an atmospheric measurement, and the linear interpolation between adjacent values. The residuals are randomly distributed and amount typically to 0.007%, which translates to a 0.006 K uncertainty on each datum point during a scan.

During the scans we relied on mechanical stops to assure that the same zenith angles could be reliably repeated. In 1987 pointing angles were measured before (or after) each series of scans. The measurement uncertainty is less than 5 arcminutes, and the values are consistent within this measuring error. The uncertainty translates into a 0.5% error (±0.005 K) in the value of $T_{A,atm}$ measured at 30°, and 0.4% error (±0.004 K) at 40°. In 1988 we used an electronic clinometer to read and record the zenith angle at the same time as we were taking data. For the analysis we used the angle given by the clinometer output; the precision of the reading was limited by the resolution of the recording system, and amounts to ±5'. This translates to a 0.6% error for the measurements at 30°, and a 0.5% error for the measurements at 40°.

The galactic signal was computed from measurements and models and subtracted from the data. The analysis suggests an uncertainty of less than 0.008 K in the model used. This error would imply an uncertainty of 0.04 K for the atmospheric measurements at 30°, and 0.02 K at 40°.

Changes in receiver system temperature or calibration coefficient that correlate with changes in receiver position have been measured by firmly attaching a piece of eccosorb at ambient temperature to the horn and then moving the radiometer, while the output signal was monitored. The output increased by +0.008±0.004 K when the radiometer was moved from the vertical to the 30° and 40° positions. The construction of the horn and of the horn/amplifier interface (aluminum pieces firmly bolted together) suggests that insertion loss changes before the first amplifier are not the cause of the observed effect. Although this is probably due primarily to changes in the target (if the emissivity of the target were to change from 0.9995 to 0.9992, a change of less than 3 dB in the reflectivity of the target , it would produce the effect we see), we can use it to set limits on the effect of changes in system temperature and calibration constant. The measured limits imply a system-temperature-change-induced uncertainty of 0.004 K, or a calibration constant uncertainty of 0.003%. The largest uncertainty on $T_{A,atm}$ would come from a system temperature change, and we will use this assumption in our error estimate.

Using the results of Table 4 and adding systematic and statistical errors in quadrature, we can obtain a final value and uncertainty for the atmospheric antenna temperature:

$$T_{A,atm} = 0.898 \pm 0.064 \text{ K} \qquad \text{(1987 data)}$$

$$T_{A,atm} = 0.955 \pm 0.055 \text{ K} \qquad \text{(1988 data)}$$

The average is obtained by weighting the averages of each pointing angle according to their systematic uncertainty. The error bars for the 30° and 40° pointing are quite different; any way of combining the errors would reduce the estimate of the overall uncertainty. Since the error bars are not independent from each other, we took the smallest set of errors in table 5, rather than combining them together statistically.

d) *Comparison with models*

The atmospheric antenna temperature as a function of frequency, altitude, and water vapor content can be computed from existing models (Costales *et al.* 1986, Liebe 1985). In these models, emission and absorption at 3.8 GHz is mostly due to the continuum of the oxygen molecules, with an extremely weak contribution from the wings of the water line at 22 GHz. We used the measurements of atmospheric antenna temperature at 10 and 90 GHz that were done simultaneously with the 3.8 GHz zenith sky measurements to estimate the atmospheric water vapor content. Under the observed conditions, the models predict atmospheric antenna temperatures at 3.8 GHz between 0.83 and 0.90 K. A new, refined model of atmospheric emission (Danese and Partridge 1989) predicts antenna temperatures between 0.93 K and 0.98 K.

The measured atmospheric temperatures tend to be on or beyond the upper limit of the predicted values, possibly suggesting that the model we are using, which provides a very good fit to the high-frequency data, underestimates the contribution of the O_2 continuum. The improved agreement between data and the Danese and Partridge model could be due to their use of a larger value for the parameters describing the O_2 continuum. Measurement-to-measurement variations (typically 0.04-0.05 K) are somewhat larger than what we would expect from short-time-scale variations of the atmospheric water vapor content (up to 0.03 K, according to Danese (1987)) but the additional scatter is well within the error bars of the overall measurement. During CBR measurements (see section VIII) the difference between the zenith sky and the reference cold load was extremely stable on time scale of tens of minutes; since the main source of temporal variation in this difference is the atmospheric emission, the stability of the signal suggests that whatever variations we see in our measurements of atmospheric antenna temperature either is due to local clouds, or do not originate in the atmosphere.

VII. COLD LOAD CALIBRATOR

The cold load calibrator (CLC) used for the 1987 experiment has been described previously (Smoot *et al.* 1985) and has not been modified; it consists of a slab of Eccosorb (emissivity > 0.999 at microwave frequencies) covering the bottom of a large (70 cm wide, 150 cm deep) Dewar container, which is filled with liquid helium (LHe), so that the Eccosorb is completely submerged; its radiometric temperature is, to very good approximation, the temperature of the cryogenic liquid in it. We measured the boiloff temperature of the LHe by measuring the ambient pressure inside the CLC, and converting it to temperature via standard tables (Duriex and Rusby 1983)After the measurements in White Mountain and during the winter 1987 in Berkeley, we made tests and measurements, trying to better understand its performance. These tests included measuring the change in antenna temperature of the cold load when the distance between the radiometer and the eccosorb was changed. The test was repeated for different temperatures of the cold load (ambient, LN and LHe). The tests yielded an upper limit on the amplitude of the coherent reflection. The results of the tests and calculations are summarized in Table 6, as correction to the temperature of the CLC.

In 1988 we used a new CLC. Its design, construction and radiometric performances are described elsewhere (Bensadoun *et al.* 1990). The main differences between the new and old CLC are the increase in diameter, the larger thickness of the microwave absorber, the stiffening of the radiometric wall and the elimination of many small steps and discontinuities in it, and the replacement of the mechanical shutter with IR-blocking, teflon impregnated glass cloth windows. Table 7 gives the radiometric temperature of the new CLC.

VIII. ZENITH SKY TEMPERATURE

Measurements of the zenith sky temperature were done (in 1987) during the nights of 14 and 15 Sept (UT) on "high" gain, and (in 1988) during the nights of 16 and 17 Sept on "high" gain and 19 Sept. (UT) on "low" gain. The receiver viewed alternately three different loads during the measuring routine: the vertical sky, an ambient temperature eccosorb target (used as a warm load), and the CLC. The loads were alternated according to a fixed scheme: sky, CLC (with radiometer turned upside down), sky, warm load. Each sequence of 4 positions constitutes a scan. Movement from one position to the next took less than 6 seconds, so that most of the time (32 sec) allocated for each position could be used to integrate the signal.

After accounting for the receiver calibration constant, we subtract the galactic signal and add the antenna temperature of the CLC, obtaining, with r.m.s. variation:

$$T_{A,CBR}+T_{A,atm} = 3.333 \pm 0.031 \text{ K} \quad \text{(1987 data)}$$

$$T_{A,CBR}+T_{A,atm} = 3.600 \pm 0.007 \text{ K} \quad \text{(1988 data)}$$

After subtracting the atmospheric and galactic signals, and adding the antenna temperature of the cold load, we obtain the results summarized in Table 8.

Changes in receiver system temperature have been measured by attaching a piece of eccosorb (at ambient temperature) to the horn, and measuring the output signal change when the radiometer was moved. The tests indicated that the receiver output changed by -0.030±0.020 K (in 1987) and by +0.012±0.008 K (in 1988), when it was rotated upside-down, with the uncertainty coming mostly from spread of experimental results. Although this is probably due primarily to changes in the target, or in the calibration constant, we adopt it for our measurement of ΔT_{sys}. If we use this value as a measurement of gain variations, as stated in eq. (3), then the uncertainty introduced in our result would become just 0.009 K.

Galactic corrections for the vertical sky brightness during CBR measurements were computed from the model, and subtracted from each single scan. The galactic signal ranged from 0.053 to 0.061 K in 1987 and from 0.058 to 0.071 K in 1988. We took as uncertainty 0.01 K, to account for both model and data uncertainties. Cold load temperature uncertainties are listed in Table 7.

In 1988 the statistical spread of the data is small, as shown in Table 9, and contributes negligibly to the total experimental uncertainty.

IX. TEMPERATURE OF THE CBR; RESULT AND DISCUSSION

Combining eq. (2) and (3) gives:

$$T_{A,CBR} = G\,(S_{zenith} - S_{load}) + T_{A,load} - \Delta T_{sys} - T_{A,galaxy} - T_{A,ground} - T_{A,atm} \quad (4)$$

We now have all the elements to compute the temperature of the CBR. From eq. (4) and Table 9, we can write: $T_{A,CBR} = 2.46 \pm 0.09$ K or, converting to thermodynamic temperature:

$$T_{CBR} = 2.56 \pm 0.09 \text{ K} \quad \text{(1987 data)}$$

Using the data from the 1988 experimental campaign, we have instead: $T_{A,CBR} = 2.62 \pm 0.07$ K or, converting to thermodynamic temperature:

$$T_{CBR} = 2.71 \pm 0.07 \text{ K} \quad \text{(1988 data)}$$

where the errors come from the data in Table 9.

These results are in statistical agreement with the weighted average of all other recent measurements of the CBR; $T_{CBR} = 2.74 \pm 0.02$ K from all measurements below 90 GHz, and $T_{CBR} = 2.63 \pm 0.04$ K from all low frequency measurements (Levin 1989); the 1988 datum however is in only marginal agreement with the 1987 one reported here, or with our measurement at 3.7 GHz (De Amici *et al.* 1988), of $T_{CBR} = 2.59 \pm 0.13$ K.

If we combine the results of all three years and weight them according to their overall error, we obtain:

$$T_{CBR} = 2.64 \pm 0.07 \text{ K}$$

where the error has been taken to be the uncertainty on the most precise measurement.

The three data points are not totally independent from each other; the atmospheric and galactic models used in the analysis (and the errors introduced by them) are the same from year to year. Nevertheless, the difference between the quantity ($T_{A,CBR}+T_{A,atm}$) as measured in 1987 and 1988, is 267±64 mK. The error bar includes (added in quadrature) the uncertainties for the cold load temperature, the galactic signal, the sidelobes and the position dependent offset. Even considering the different atmospheric antenna temperature between the two years (as reported in table 4a,b), the difference is quite large and statistically unlikely (3.2σ). On the other hand, the 1986 and 1987 results are in excellent agreement with each other. The main difference between the 1986 and 1987 experiments and the 1988 one is the use of a new CLC.

The 1986 measurements yielded an atmospheric emission in marginal agreement with the standard model of the time: however it should be noted that successive refinements of that same model (Danese and Partridge 1989) have led to predictions of even higher antenna temperature. In 1987 the atmospheric antenna temperature was slightly lower than measured in 1988. The only instrumental effect that could reconcile all the data is a large change in system noise (or calibration constant) that has gone undetected, and that affects data from different years in a different way. We compared the signal from a piece of LN-soaked absorber, held over the horn, with that from the LN-filled CLC, and found them to be within 0.03 K from each other. However, the antenna temperature of the LN-soaked absorber changes very rapidly as the liquid drips away, cooling the antenna and modifying its transmission properties. The uncertainty in the measurement is many times the measured effect.

RFI could be the cause of the abnormally large spread of the data, and of the yearly variation of sky temperature that we observe; we took every conceivable precaution to identify and resolve the problem, but a definitive resolution of the RFI problem will only be obtained by taking data from a remote civilization-free location.

These results set a very tight constraint on the shape of the spectrum of the CBR below 10 GHz, confirming the measurements at 2.5 GHz (Sironi and Bonelli 1986) and 4.75 GHz (Mandolesi *et al* 1986) and possibly relegating any chance of a significant distortion to the spectral region below 1 GHz, where high precision observations and measurements are made difficult by the overwhelmingly strong and spatially varying galactic emission.

X. ACKNOWLEGMENTS

This research was funded in part by the Director, Office of Energy Research, Office of High Energy and Nuclear Physics, Division of High Energy Physics of the U.S. Department of Energy under Contract DE-AC03-76SF00098 and by the National Science Foundation Grant No. AST 8406187. We wish to thank the crew and staff of the White Mountain Research Station, and Faye Mitschang, John Gibson, Armando Meuti, Larry Levin, Jon Aymon, Jenny Hwang, Barron Chugg for their help, and Dr. G. De Zotti for his careful reading of the manuscript.

Table 1 - Relevant parameters of the 3.8 GHz receiver

center frequency	3.78 GHz	measured
wavelength	7.9 cm	computed
bandwidth	105 MHz	measured
system noise	84±1 K [(a)]	measured w/cold and warm loads
sensitivity	5.8 mK/sec$^{1/2}$	theoretical
	13 mK/sec$^{1/2}$	measured w/ambient target
beamwidth (HPBW)	16°	measured
RF gain	68 dB	measured
DC gain	400x/1500x[(b)]	measured (1987)
	800x/1760x[(b)]	measured (1988)
azimuth	90.0±0.1°	measured

[(a)] peak-to-peak variation of measured values

[(b)] switchable

Table 2 - Position-target sequence for atmospheric measurements

radiometer position	target	gain status
40° West of vertical	sky for cold reference load [a,b]	low
40° West of vertical	warm eccosorb [b]	low
40° West of vertical	sky 40° West position	high
30° West of vertical	sky 30° West position	high
vertical	zenith sky [b]	high
30° East of vertical	sky 30° East position	high
40° East of vertical	sky 40° East position	high

[a] measured signal was corrected to zenith sky signal

[b] this position was repeated at the end of each measurement

Table 3 - Pointing angles for atmospheric measurements

(all angles are measured from vertical to within ±5')

	zenith	30° E	40°E	30°W	40°W
1987 measurements	0°32'E	30°05'	39°57'	29°34'	39°12'
1988 measurements	0°27' E	29°22'	39°11'	30°32'	40°33'

Table 4a - Results of 1987 atmospheric measurements (only statistical error are quoted).

day	time [UT] from:	to:	scans	average signal and error[K]	
11	10:48	11:00	8	0.896	0.018
11	11:20	11:37	6	0.890	0.049
14	8:57	9:37	11	0.926	0.086
15	8:12	8:53	13	0.950	0.056
16	8:25	9:22	18	0.917	0.048
18	7:09	7:22	5	0.935	0.075
18	8:27	8:40	6	0.908	0.016
18	9:16	9:32	6	0.825	0.020
18	10:10	10:26	6	0.879	0.021
20	8:19	8:35	6	0.859	0.010
average of the 10 measurements (and error):				0.898	0.012

Table 4b - Results of 1988 atmospheric measurements (only statistical error are quoted).

day	time [UT] from:	to:	scans	average signal and error [K]	
7	9:31	9:54	7	0.943	0.018
9	8:34	9:16	11	0.951	0.019
10	6:13	6:28	4	0.943	0.038
14	4:55	5:25	7	0.950	0.019
14	5:31	5:50	6	0.994	0.011
14	10:06	10:32	7	0.954	0.025
16	3:35	4:37	10	0.924	0.023
16	5:32	6:12	10	0.946	0.018
16	6:54	7:04	3	0.976	0.040
16	10:36	11:03	7	1.003	0.015
17	7:57	8:34	10	0.924	0.023
17	9:32	9:52	5	0.985	0.027
17	11:51	12:19	7	0.977	0.020
	average of the 13 measurements (and error):			0.959	0.008

Table 5a - Error budget for atmospheric antenna temperature evaluation during 1987 experiment

quantity	amount	kind of error	uncertainty on $T_{A,atm}$ [K] at 30°	at 40°
spread of data	±0.037 K	statistical	0.037	0.037
atmospheric scale height	6±2 km	systematic	0.001	0.001
atmosph. kinetic temperature	260±20 K	systematic	0.001	0.001
diffracted earth radiation	(see text)	systematic	0.036-0.042	0.024-0.030
pointing error	± 5 '	systematic	0.007	0.005
error on value of gain	0.8%	systematic	0.008	0.008
error due to gain drift	0.006 K	systematic	0.036	0.018
saturation corrections	0.8%	systematic	0.008	0.008
beam pattern	±3° HPBW	systematic	0.020	0.020
galactic correction	(see text)	systematic	0.040	0.030
radiometer offset change	±0.003 K	systematic	0.018	0.009
RFI	±0.002 K	systematic	0.012	0.006
total systematics			0.065-0.069	0.050-0.053
total errors			0.075-0.078	0.062-0.065

Table 5b - Error budget for atmospheric antenna temperature evaluation during 1988 experiment

quantity	amount	kind of error	uncertainty on $T_{A,atm}$ [K]	
			at 30°	at 40°
spread of data	±0.027 K	statistical	0.027	0.027
atmospheric scale height	6±2 km	systematic	0.001	0.001
atmosph. kinetic temperature	260±20 K	systematic	0.001	0.001
diffracted earth radiation	(see text)	systematic	0.036-0.042	0.024-0.030
pointing error	± 5 '	systematic	0.007	0.005
error on value of gain	0.83%	systematic	0.008	0.008
error due to gain drift	0.006 K	systematic	0.036	0.018
saturation corrections	0.3%	systematic	0.003	0.003
beam pattern	±3° HPBW	systematic	0.020	0.020
galactic correction	(see text)	systematic	0.030	0.024
radiometer offset change	±0.004 K	systematic	0.024	0.012
RFI	±0.002 K	systematic	0.012	0.006
total systematics			0.067-0.072	0.045-0.049
total errors			0.072-0.077	0.054-0.057

Table 6 - Radiometric temperature of the cold load in 1987; ambient pressure was 487 mm Hg

quantity	contribution to antenna temperature [K]	error [K]
emission of cryogenically cooled target	3.692	0.004
emission of windows and gas	0.007	0.005
emission loss of walls	0.014	0.007
emission of bellows and shutter	0.009	0.007
incoherent reflection	0.020	0.010
coherent reflection	0.000	0.035
total	3.742	0.038

Table 7 - Radiometric temperature of the cold load in 1988; ambient pressure was 484 mm Hg

quantity	contribution to antenna temperature [K]	error [K]
emission of cryogenically cooled target	3.686	0.004
emission of windows and gas	0.003	0.002
emission loss of walls	0.007	0.006
incoherent reflection	0.006	0.003
coherent reflection	0.000	0.030

total	3.702	0.031

Table 8 - Difference between vertical sky and cold load calibrator antenna temperatures, after correcting for galactic and atmospheric signal as discussed in text, but before subtracting sidelobes or offset changes.

Final value is the average of all data points, with rms uncertainty

day and time (UT)	number of data points	difference [K] average	r.m.s.
14 Sep 1987 01:02-01:49	21	-1.270	0.020
14 Sep 1987 07:44-08:29	26	-1.312	0.034
15 Sep 1987 07:45-07:57	5	-1.324	0.017
average for 1987 [a]		-1.302	0.031
16 Sep 1988 07:26-08:19	25	-1.052	0.004
16 Sep 1988 09:28-10:15	22	-1.060	0.004
17 Sep 1988 11:20-11:27	7	-1.061	0.004
17 Sep 11:28-11:36	4	-1.054	0.004
19 Sep 08:17-08:	5	-1.050	0.008
average for 1988		-1.056	0.007

[a] data have been inversely weighted by the uncertainty in the atmospheric correction used

Table 9 - Summary of data for measurements of antenna temperature of CBR.

quantity	1987		1988	
	amount [K]	error [K]	amount [K]	error [K]
atmospheric temperature	0.898[a]	±0.064	0.955	±0.055
sidelobes	0.010	±0.005	0.007	±0.004
position dependent output change	-0.030	±0.020	0.012	±0.008
cold load temperature	3.742	±0.038	3.697	±0.031
galactic emission	0.057[a]	±0.010	0.065[a]	±0.010
difference between sky and cold load	-0.347[a]	±0.008	-0.037[a]	±0.001
$T_{a,CBR}$ (according to eq. 4)	2.460	±0.079 [b]	2.621	±0.065 [b]
		±0.145 [c]		±0.119 [c]

(a) these are representative values, which have been adjusted so that their total reflects the average given in the text.

(b) errors have been added in quadrature

(c) errors have been added linearly

References

Bensadoun M., *et al.*, 1990, *Rev. Sci. Inst.,* to be submitted

Bersanelli, M., *et al.*, 1989, *Ap. J.*, **339**, 632.

Costales, J., *et al.*, 1986, *Radio Science*, **21**, 47.

Danese, L., 1987, priv. comm.

Danese, L. and De Zotti, G., 1982, *Astron. Astroph.,* **107**, 39

Danese, L. and Partridge, R.B., 1989, *Ap. J.*, **342**, 604

De Amici, G., *et al.*, 1988, *Ap. J.*, **329**, 556.

De Amici, G., *et al.*, 1985, *Ap. J.*, **298**, 710.

De Zotti, G., 1986

Duriex, M. and Rusby, R.L., 1983, *Metrologia*, **19**, 67

Haslam, C.G.T., Salter, C.J., Stoffel, H., and Wilson, W.E., 1982, *Astr. Astroph. Suppl. Ser.*, **47**, 1.

Hayakawa, S. *et al*, 1987, *Publ Astron Soc Japan*, **39**, 941

Kogut, A., *et al.*, 1990, *Ap. J.*, in press.

Levin S.M., *et al.*, 1988, *Ap. J.*, **334**, 14.

Levin S.M., *et al.*, 1989, in: E. Norman (edt.) *Particle Astrophysics: Forefront Experimental Issues,* (World Scientific, Singapore)

Liebe, H.J., 1985, *Radio Science,* **20**, 1069.

Matsumoto T., *et al*, 1988, *Ap. J.*, **329**, 567

Mandolesi, N., *et al.*, 1986, *Ap.J.*, **310**, 561

Sironi, G. and Bonelli, G., 1986, *Ap.J.*, **311**, 418.

Smoot, G., *et al.*, 1985, *Ap.J. Lett.*, **291**, L23

Smoot, G., *et al.*, 1987, *Ap.J. Lett.*, **317**, 45

Smoot, G., *et al.*, 1988, *Ap. J.,* **331**, 653

Figure captions

1 - Results of differential galactic drift scans at 36° declination, and prediction of a similar scan obtained from extrapolation of the map at 408 MHz (Haslam *et al.* 1982) and of a compilation of sources at 2.5 GHz, and fitted to the measured antenna beam pattern. The profile shown is for spectral index of 2.75 for synchrotron radiation, and 2.1 for HII radiation. Experimental data (*filled circles*) have been corrected for ground contribution and binned in 5-minute intervals (≈28 data points/bin). Error bars shown are typical.

2 - Recent measurements of the temperature of the CBR between 1 and 11 GHz (for references see [e.g.] Kogut *et al* 1989)

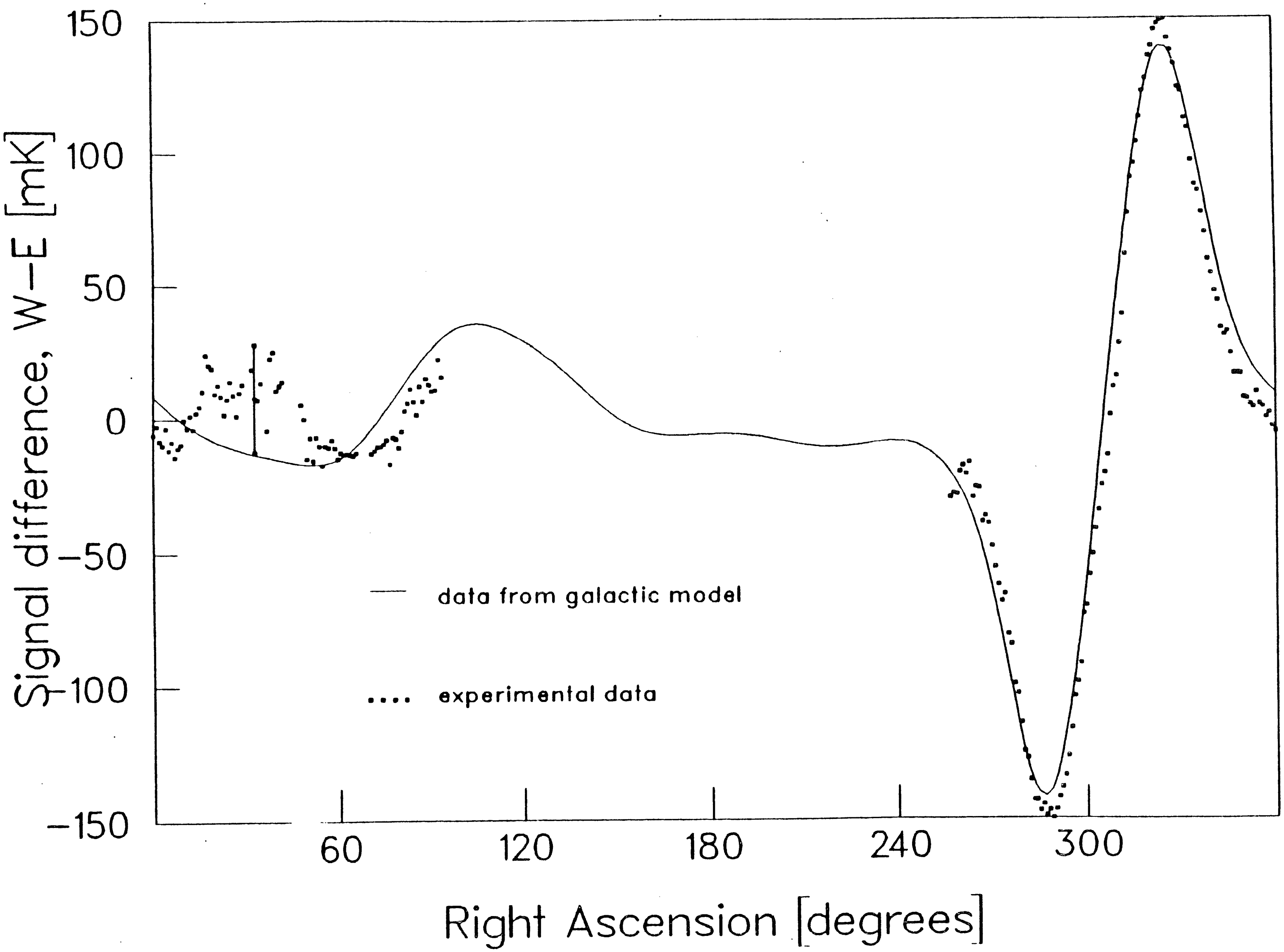
Signal difference, W−E [mK]
150
100
50
0
−50
−100
−150
60
120
180
240
300
Right Ascension [degrees]
data from galactic model
experimental data

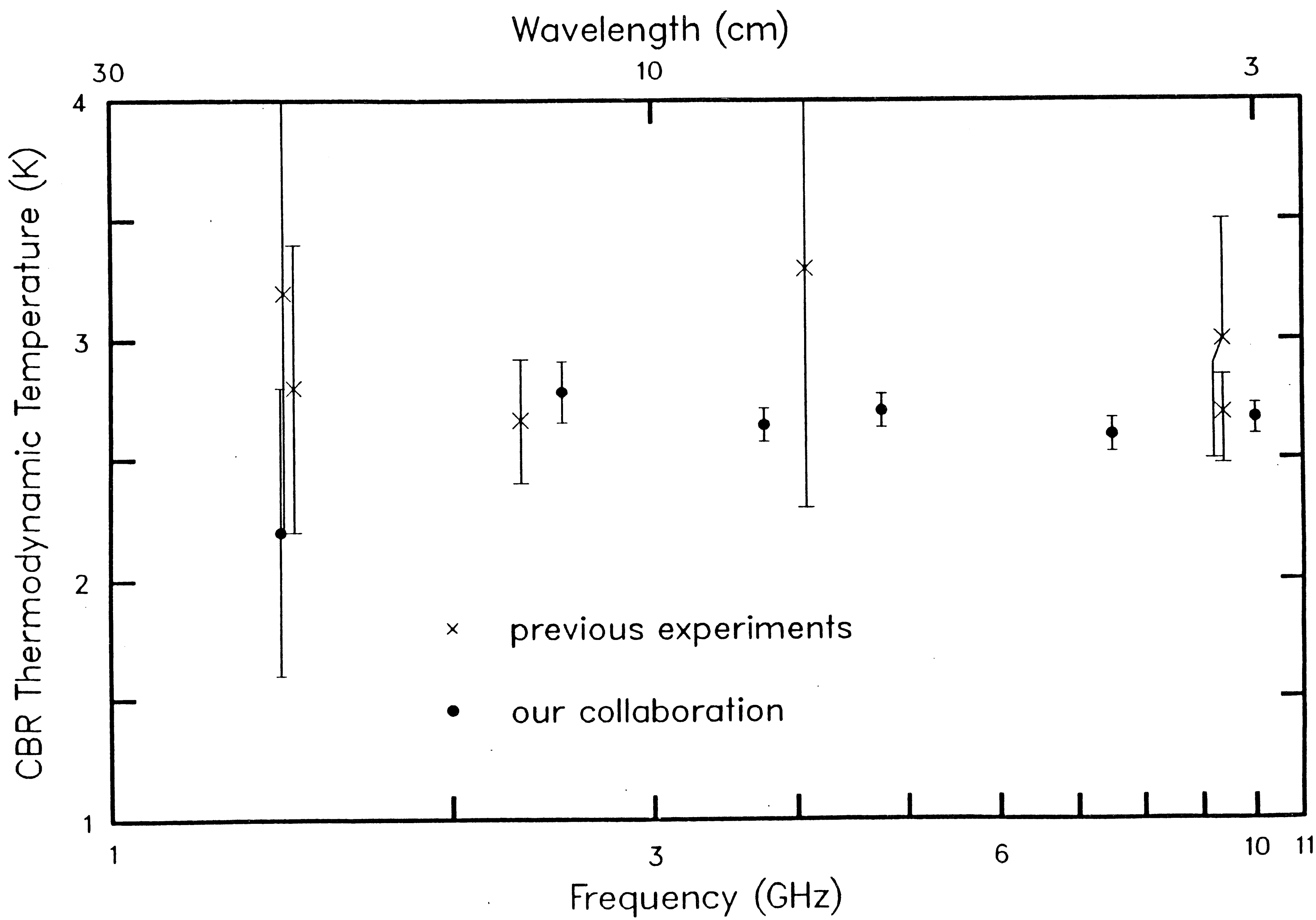
Wavelength (cm)
30
10
3
CBR Thermodynamic Temperature (K)
4
3
2
1
× previous experiments
● our collaboration
1
3
6
10
11
Frequency (GHz)